

A Radix-4 Chrestenson Gate for Optical Quantum Computation

Kaitlin N. Smith, Tim P. LaFave Jr., Duncan L. MacFarlane, and Mitchell A. Thornton

Quantum Informatics Research Group

Southern Methodist University

Dallas, TX, USA

{knsmith, tlafave, dmacfarlane, mitch} @smu.edu

Abstract—A recently developed four-port directional coupler used in optical signal processing applications is shown to be equivalent to a radix-4 Chrestenson operator, or gate, in quantum information processing (QIP) applications. The radix-4 qudit is implemented as a location-encoded photon incident on one of the four ports of the coupler. The quantum informatics transfer matrix is derived for the device based upon the conservation of energy equations when the coupler is employed in a classical sense in an optical communications environment. The resulting transfer matrix is the radix-4 Chrestenson transform. This result indicates that a new practical device is available for use in the implementation of radix-4 QIP applications or in the construction of a radix-4 quantum computer.

Index Terms—quantum information processing; quantum photonics; qudit;

I. INTRODUCTION

In the field of quantum computing, theory has been well developed over the last half-century. There is still room for the discovery of new operators and algorithms, but current work is enough to show the potential that quantum methods have for solving some of the most difficult scientific problems. Unfortunately, the physical implementations for QIP have not advanced as rapidly as the theory. Since a standard platform has not been chosen for the quantum computer (QC), efforts have been divided among many competing technologies with quantum optics being one of the more promising physical realizations. This work hopes to contribute a new component to the already well-established optical quantum computing library.

The four-port directional coupler is an optical component shown theoretically to act as a quantum gate that can place a radix-4 photon encoded qudit into a state of equal superposition. The gate realized optically is known as the radix-4 Chrestenson gate, and it is derived from the generalized radix- p Chrestenson transformation. This operator is significant to the field of QIP due to the need to put quantum information in a state of superposition for quantum algorithm execution. A description of the four-port coupler as well as a demonstration of its capabilities as a quantum optics operator will be shown mathematically in this work.

This paper will proceed as follows. A brief summary of important QIP concepts, details of the Chrestenson gate, and information about quantum optics is provided in Section II. The four-port directional coupler, the component of interest,

is described in Section III followed by the realization of the coupler with optical elements including its fabrication and characterization in Section IV. Demonstration of the four-port coupler as a radix-4 Chrestenson gate is presented in Section V and a summary with conclusions is found in Section VI.

II. QUANTUM THEORY BACKGROUND

A. The Qubit vs. Qudit

The quantum bit, or qubit, is the standard unit of information for radix-2, or base-2, quantum computing. The qubit models information as a linear combination of two orthonormal basis states such as the states $|0\rangle$ and $|1\rangle$. $|0\rangle$ and $|1\rangle$ are Dirac notation representations where $|0\rangle = [1 \ 0]^T$ and $|1\rangle = [0 \ 1]^T$, respectively. The qubit differs from the classical bit by its ability to be in a state of superposition, or a state of linear combination, of all basis states. There are theoretically an infinite number of states for a qubit while in a state of superposition

$$|\Psi\rangle = x|0\rangle + y|1\rangle = [x \ y]^T \quad (1)$$

where x and y are complex values, $c \in \mathbb{C}$, such that $c = a + ib$ where i is an imaginary number, $i^2 = -1$. For the qubit $|\Psi\rangle$, the probability that $|\Psi\rangle = |0\rangle$ is equal to $x^*x = |x|^2$ and the probability that $|\Psi\rangle = |1\rangle$ is equal to $y^*y = |y|^2$ where the symbol $*$ indicates a complex conjugate. The total probability of occupying either one basis state or the other must total to 100%, so the inner product, or dot product, of $|\Psi\rangle$ with itself must equal 1. In other words, $x^*x + y^*y = 1$. Once a qubit is measured, it collapses into a basis state as defined by the eigenvectors of the measurement operator. The measurement operation causes a qubit's state of superposition to be lost.

Qubits are the current standard for encoding data in QIP, but it is possible to have a quantum system of higher order. A quantum unit of dimension, or radix, $p > 2$ is referred to as a qudit. In this paper, the radix-4 qudit using four orthonormal basis states is of interest. The set of basis states used for this qudit includes the vectors $|0\rangle = [1 \ 0 \ 0 \ 0]^T$, $|1\rangle = [0 \ 1 \ 0 \ 0]^T$, $|2\rangle = [0 \ 0 \ 1 \ 0]^T$, and $|3\rangle = [0 \ 0 \ 0 \ 1]^T$. Just like the radix-2 qubit, the radix-4 qudit is not limited to having the value of only one of its four possible basis states. The qudit is capable of existing in a

linear combination, or a state of superposition, of all four basis states, as demonstrated by

$$|\Phi\rangle = v|0\rangle + x|1\rangle + y|2\rangle + z|3\rangle = [v \ x \ y \ z]^T \quad (2)$$

where v , x , y , and z are complex values. These coefficients can be multiplied by their respective complex conjugates in order to derive the probability that the radix-4 qudit is in a particular basis state. The basis state probabilities of $|\Phi\rangle$ must sum to 100%, so $v^*v + x^*x + y^*y + z^*z = 1$.

For a radix-4 quantum system to be physically realized, a methodology must exist for encoding four distinct qudit basis states. In [5], Rabi oscillations are utilized to create radix- p quantum systems. Orbital angular momentum (OAM) states of light could also be used to encode the qudit [16]. In this paper, a radix-4 quantum state will be created using the location of light as the information carrier. This technique builds on the concept of photonic dual-rail representation of the qubit in order to physically realize qudit with a quad-rail implementation.

B. Quantum Operations

A quantum state must undergo purposeful transformations through quantum operations in order to develop meaningful information from QIP. If a quantum algorithm is modeled as a circuit, quantum operations can be viewed as quantum logic gates. Each of these gates is represented by a unique, unitary transfer function matrix, \mathbf{U} , that is characterized by the following properties:

- $\mathbf{U}^\dagger \mathbf{U} = \mathbf{U} \mathbf{U}^\dagger = \mathbf{I}_p$
- $\mathbf{U}^{-1} = \mathbf{U}^\dagger$
- $\text{Rank}(\mathbf{U}) = p$
- $|\mathbf{U}| = 1$

When considering radix- p quantum operations, or gates, the transfer function matrices will always be square matrices each of a dimension that is a power of p . Therefore, radix-4 qudit operations will have a dimension that is a power of four, 4^k , where the power, k , indicates the number of qudits transformed by an operation.

C. The Chrestenson Gate

The power of QIP lies in the ability for a quantum state to be in superposition. In radix-2 quantum computation, the Hadamard gate

$$\frac{1}{\sqrt{2}} \begin{bmatrix} 1 & 1 \\ 1 & -1 \end{bmatrix} \quad (3)$$

is an important operator used to put a qubit in a state of superposition so that it has equal probability of being observed, or measured, as either $|0\rangle$ or $|1\rangle$. Quantum operators exist for many different computation bases that achieve equal superposition among the corresponding basis states. These operators are derived using the discrete Fourier transform on Abelian groups. General theory of Fourier transforms on Abelian

groups is outlined in [6] as well as in [7]. The multiple-valued generalization of the radix-2 quantum Hadamard gate and its transfer matrix is composed of discretized versions of the orthogonal Chrestenson basis function set [7]. This gate is generally referred to as the Chrestenson gate [8]. The generalized radix- p Chrestenson transfer function is represented with a matrix in the form of

$$\frac{1}{\sqrt{p}} \begin{bmatrix} w^{0(0)} & w^{1(0)} & \dots & w^{(p-1)0} \\ w^{0(1)} & w^{1(1)} & \dots & \vdots \\ \vdots & \vdots & \ddots & \vdots \\ w^{0(p-1)} & \dots & \dots & w^{(p-1)(p-1)} \end{bmatrix}. \quad (4)$$

Eq. 4 contains elements w^k based on the p -th roots of unity found on the unit circle in the real and imaginary plane according to $w = \exp(i2\pi/p)$ [7], [8]. The resulting values satisfy $(w^k)^p = 1$ as roots of unity. Using the fourth roots of unity, $\exp[(i2\pi/4)*1] = i$, $\exp[(i2\pi/4)*2] = -1$, $\exp[(i2\pi/4)*3] = -i$, and $\exp[(i2\pi/4)*4] = 1$, in the general form in Eq. 4, the radix-4 Chrestenson gate transfer matrix of is derived as

$$\mathbf{C4} = \frac{1}{\sqrt{4}} \begin{bmatrix} 1 & 1 & 1 & 1 \\ 1 & i & -1 & -i \\ 1 & -1 & 1 & -1 \\ 1 & -i & -1 & i \end{bmatrix}. \quad (5)$$

The radix-4 Chrestenson gate (C4), allows a radix-4 qudit originally in a basis state to evolve into a state of equal superposition. The example below shows how the radix-4 qudit $|a\rangle = |0\rangle$ evolves to $|b\rangle = \frac{1}{2}|0\rangle + \frac{1}{2}|1\rangle + \frac{1}{2}|2\rangle + \frac{1}{2}|3\rangle$ after passing through the C4 transform

$$\mathbf{C4}|a\rangle = |b\rangle,$$

$$\mathbf{C4}|0\rangle = \frac{1}{\sqrt{4}} \begin{bmatrix} 1 & 1 & 1 & 1 \\ 1 & i & -1 & -i \\ 1 & -1 & 1 & -1 \\ 1 & -i & -1 & i \end{bmatrix} \begin{bmatrix} 1 \\ 0 \\ 0 \\ 0 \end{bmatrix} = \frac{1}{2} \begin{bmatrix} 1 \\ 1 \\ 1 \\ 1 \end{bmatrix},$$

$$\mathbf{C4}|0\rangle = \frac{1}{2} [|0\rangle + |1\rangle + |2\rangle + |3\rangle].$$

If $|a\rangle = |3\rangle$, the radix-4 qudit would evolve to $|b\rangle = \frac{1}{2}|0\rangle - \frac{1}{2}i|1\rangle - \frac{1}{2}|2\rangle + \frac{1}{2}i|3\rangle$

$$\mathbf{C4}|3\rangle = \frac{1}{\sqrt{4}} \begin{bmatrix} 1 & 1 & 1 & 1 \\ 1 & i & -1 & -i \\ 1 & -1 & 1 & -1 \\ 1 & -i & -1 & i \end{bmatrix} \begin{bmatrix} 0 \\ 0 \\ 0 \\ 1 \end{bmatrix} = \frac{1}{2} \begin{bmatrix} 1 \\ -i \\ -1 \\ i \end{bmatrix},$$

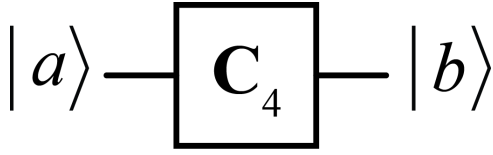


Fig. 1. Symbol of the radix-4 Chrestenson gate, C4.

$$\mathbf{C4}|3\rangle = \frac{1}{2} [|0\rangle - i|1\rangle - |2\rangle + i|3\rangle].$$

The schematic symbol for the C4 gate is pictured in Fig. 1.

D. Quantum Optics

Optical quantum implementations are among the more successful physical realizations of quantum states. In these systems, orthogonal basis states can be encoded into photon OAM states, polarization, or location, and the state can easily evolve by passing through linear optical elements. The photon resists coupling to other objects in its environment, allowing it to maintain its quantum state and not decohere for long periods of time [9]. Additionally, the ability to maintain coherence enables the photon to travel great distances at room temperature, making it a good candidate for long-haul quantum information transmission.

Although photons offer the benefit of state stability in QIP applications, their failure to interact with their surroundings prevents them from coupling with each other. Photon-to-photon interaction is difficult, limiting the development of reliable multi-qubit, or multi-qudit in higher radix systems, gate implementations. Without operations such as the controlled-NOT (CNOT) gate or the controlled-phase gate, a functional quantum computer cannot exist.

It was once thought that photonic quantum computation was unachievable without nonlinear optical elements, but the presentation of the KLM protocol in [10] improved the outlook for quantum optics. In that work, a methodology for implementing photonic multi-qubit operations using linear optics was introduced. These multi-qubit photonic gates, however, are unfortunately limited by probabilistic operation. Currently, the two-qubit CNOT operation can only work 1/4 of the time when implemented with linear optical elements in the best case scenario [11].

The subject of this paper is a photonic radix-4 Chrestenson gate. Since this quantum operator is formed from linear optical elements and transforms a single qudit at a time, the gate is theoretically deterministic in nature.

III. THE FOUR-PORT DIRECTIONAL COUPLER

The four-port directional coupler is an optical component introduced and described in [4]. This device is composed of four inputs and four outputs where the input and output are referred to by their orientation on the component of either W, N, E, or S. When a single beam is sent into one of the coupler inputs, the component routes a fraction of the original signal to each of the four outputs. This beam division is caused by the transmission and reflection of signals within the coupler.

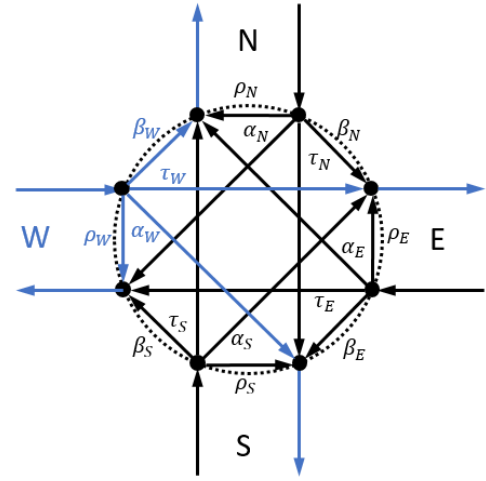


Fig. 2. Signal flow for four-port directional coupler with input at W.

Each fraction of the input beam seen at an output corresponds to one of the following components of the original signal: a reflected component ρ , a transmitted component τ , a right-directed component α , and a left-directed component β . An illustration of signal flow of the four-port directional coupler can be seen in Fig. 2. This image is recreated from a figure included in [4].

Fig. 2 demonstrates in blue a signal entering the four-port coupler from the W port and exiting the component from the W, N, E, and S ports. The output signals are generated by ρ_W , β_W , τ_W , and α_W , respectively. Whenever a single input enters the component, all four coupling coefficients are generated to produce four outputs. The coupling coefficients produced with a particular port input can be derived with the coupling coefficient matrix,

$$\begin{bmatrix} \rho_W & \alpha_N & \tau_E & \beta_S \\ \beta_W & \rho_N & \alpha_E & \tau_S \\ \tau_W & \beta_N & \rho_E & \alpha_S \\ \alpha_W & \tau_N & \beta_E & \rho_S \end{bmatrix}. \quad (6)$$

To produce the outputs, an input vector taking the form of $[WNES]^T$ is multiplied by the matrix in Eq. 6 to create a column vector of coupling coefficients. The produced output column vector also takes the form of $[WNES]^T$. The composition of the output vector in terms of coupling coefficients indicates what portion of the input signal contributes to an output from a port.

The four-port directional coupler does not consume nor dissipate any of the energy that is input into the component. Therefore, to conserve energy, all of the energy entering the element must be equal to the energy leaving the element. This concept leads to the creation of equations that act as conditions that must hold true for energy conservation. The 10 energy conservation equations of Eqs. 7-16, first derived in [4], use

the coupling coefficients found in the matrix of Eq. 6. These equations are:

$$\rho_W^* \rho_W + \beta_W^* \beta_W + \tau_W^* \tau_W + \alpha_W^* \alpha_W = 1, \quad (7)$$

$$\rho_N^* \rho_N + \beta_N^* \beta_N + \tau_N^* \tau_N + \alpha_N^* \alpha_N = 1, \quad (8)$$

$$\rho_E^* \rho_E + \beta_E^* \beta_E + \tau_E^* \tau_E + \alpha_E^* \alpha_E = 1, \quad (9)$$

$$\rho_S^* \rho_S + \beta_S^* \beta_S + \tau_S^* \tau_S + \alpha_S^* \alpha_S = 1, \quad (10)$$

$$\rho_W^* \tau_E + \beta_W^* \alpha_E + \tau_W^* \rho_E + \alpha_W^* \beta_E = 0, \quad (11)$$

$$\alpha_N^* \beta_S + \rho_N^* \tau_S + \beta_N^* \alpha_S + \tau_N^* \rho_S = 0, \quad (12)$$

$$\rho_W^* \alpha_N + \beta_W^* \rho_N + \tau_W^* \beta_N + \alpha_W^* \tau_N = 0, \quad (13)$$

$$\alpha_N^* \tau_E + \rho_N^* \alpha_E + \beta_N^* \rho_E + \tau_N^* \beta_E = 0, \quad (14)$$

$$\tau_E^* \beta_S + \alpha_E^* \tau_S + \rho_E^* \alpha_S + \beta_E^* \rho_S = 0, \quad (15)$$

and

$$\rho_W^* \beta_S + \beta_W^* \tau_S + \tau_W^* \alpha_S + \alpha_W^* \rho_S = 0. \quad (16)$$

The first four conditions seen in Eqs. 7-10 exist since the inner product of each produced field vector from a single input, W, N, E, and S, with itself must sum to 1 for energy conservation. The last six conditions seen in Eqs. 11-16 exist due to energy conservation that occurs whenever two inputs are present in the component. Since the coefficient vectors are orthogonal, the inner product between the two produced coupling coefficient vectors corresponding to inputs at two different ports must equal zero. There are only 6 constraints produced from sending two inputs to the four-port directional coupler because the input combinations are commutative (i.e. $AB = BA$). The cases of three inputs and four inputs into the four-port directional coupler do not create additional constraints, so they are omitted [4].

IV. PHYSICAL REALIZATIONS OF THE FOUR-PORT DIRECTIONAL COUPLER

A macroscopic realization of a four-port coupler is shown in Fig. 3. Whereas a popular implementation of a radix-2 Hadamard gate is an optical beam splitter, polarizing or not, the macroscopic four-port coupler is a unitary extension of a two-prism beam splitting cube. Here, the macroscopic four-port directional coupler is comprised of four right angle prisms, coated with an appropriate thin film, cemented together with care given to the precise mating of the four prism corners. This component has been used to demonstrate novel, four leg Michelson interferometers designed in [15].

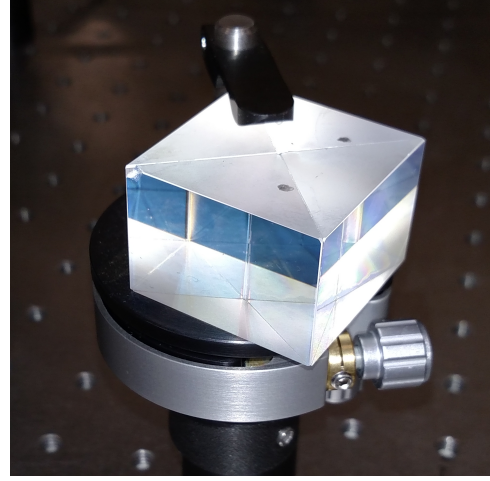


Fig. 3. Macroscopic realization of a four-port coupler.

Integrated photonic four-port couplers were previously demonstrated for applications in optical signal processing as part of a two-dimensional array of waveguides in a multi-quantum well (MQW) GaInAsP indium phosphide (InP) architecture [12], [13]. Fig. 4 shows an electron micrograph of a coupler fabricated at the intersection of two ridge waveguides.

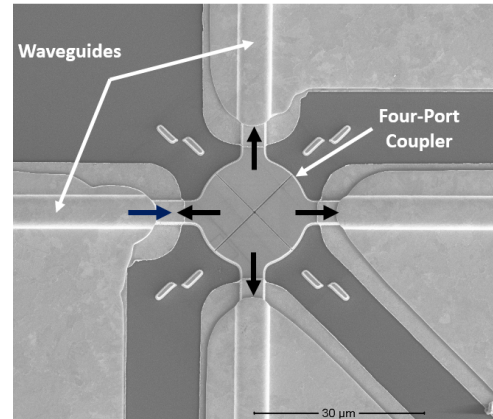


Fig. 4. Cross sectional transmission electron microscope image of a four-port coupler in MQW-InP.

The optical behavior of the four-port coupler depends on frustrated total internal reflection [14]. The evanescent field of light incident on the coupler is transferred across the width of the coupler that may be an air gap or a thin slice of dielectric. Provided the barrier width is small enough, a part of the exponentially decaying optical power of the incident light is transmitted across while the remaining optical power is reflected. Thus, a fraction of light incident on a four-port coupler may be transmitted to the ongoing waveguide, reflected to both perpendicular waveguides, or reflected back into the originating waveguide. The fractions of light in outbound waveguide are determined by the refractive indices of the waveguide and coupler materials in addition to the width of the coupler.

A. Fabrication

Fabrication of the coupler was performed in several steps using nanoelectronic processing techniques. First, coupler regions of 180 nm widths and 7 μm lengths were defined by patterning a thin metallic chromium mask layer atop the waveguides by focused ion beam (FIB) lithography. Precision alignment and orientation of the coupler to the waveguides during FIB processing was achieved with alignment markers fabricated beforehand with the waveguides using conventional microelectronic processing steps. High aspect ratio trenches were then etched using a hydrogen bromine (HBr) based [15] inductively coupled plasma (ICP) to a depth of 3.9 μm . This depth allows the coupler to fully cover optical modes confined to the quantum well region of the waveguides.

The optimal air gap width for 25% power on all output waveguides of about 90 nm was slightly smaller than the processing capability of the ICP dry etch tool for the required high-aspect ratio etch. Consequently, to meet this requirement for a wavelength of 1550 nm, alumina (Al_2O_3), with a refractive index of $n = 1.71$, was back-filled into the trench using atomic layer deposition (ALD). The resulting alumina-filled trench is shown in the composite cross-sectional transmission electron micrographs in Fig. 5.

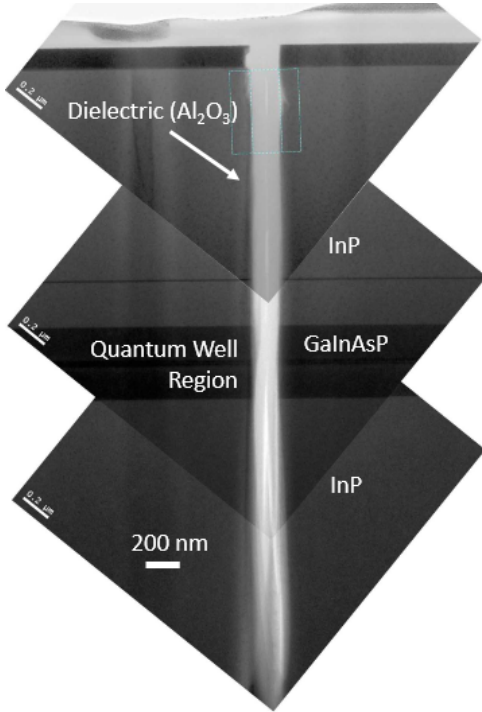


Fig. 5. Cross sectional transmission electron micrograph of a four-port coupler backfilled with alumina using atomic layer deposition.

B. Characterization

A 1550nm laser was coupled into the waveguides using a tapered lens fiber at one input port. The near-field modes of light were coupled out of the device and into another tapered lens fiber for optical power measurement to characterize the

coupling efficiency of the four-port coupler. The measured average power coefficients were $\alpha = 0.156$, $\beta = 0.140$, $\rho = 0.302$, and $\tau = 0.220$ for a measured total average coupling efficiency of 82% for the four-port coupler [12].

V. IMPLEMENTING QUDIT QUANTUM OPERATIONS WITH THE COUPLER

It is known that the Hadamard gate meant for use with a quantum qubit can be constructed from a beam splitter [9]. The radix-4 Chrestenson operation, an operation that acts on a quantum encoding using four basis states, acts on a radix-4 qudit, and the four-port directional coupler is a physical realization of this gate. In the realization of the radix-4 Chrestenson gate, the ports of the four-port directional coupler must be encoded in order to represent the four qudit basis states. In this paper, the following encoding has been chosen for the location-based scheme: port W is the $|0\rangle$ rail, port N is the $|1\rangle$ rail, port E is the $|2\rangle$ rail, and port S is the $|3\rangle$ rail.

The four-port directional coupler follows 10 energy conservation equations, Eqs. 7-16, that are algebraically nonlinear. If the radix-4 Chrestenson matrix values are substituted for the values of the coupling coefficients in Eq. 6, the energy conservation constraints are satisfied and the following matrix is generated:

$$\begin{bmatrix} \rho_W = \frac{1}{2} & \alpha_N = \frac{1}{2} & \tau_E = \frac{1}{2} & \beta_S = \frac{1}{2} \\ \beta_W = \frac{1}{2} & \rho_N = \frac{1}{2}i & \alpha_E = -\frac{1}{2} & \tau_S = -\frac{1}{2}i \\ \tau_W = \frac{1}{2} & \beta_N = -\frac{1}{2} & \rho_E = \frac{1}{2} & \alpha_S = -\frac{1}{2} \\ \alpha_W = \frac{1}{2} & \tau_N = -\frac{1}{2}i & \beta_E = -\frac{1}{2} & \rho_S = \frac{1}{2}i \end{bmatrix}$$

When a single photon, representing a qudit, is applied to one of the inputs the four-port coupler, either W, N, E, or S, energy is conserved and the radix-4 Chrestenson transform is achieved. The photon leaves the gate with equal superposition of all basis states. In other words, the photon has a 1/4 probability of being located in any of the output ports W, N, E, or S representing the basis states $|0\rangle$, $|1\rangle$, $|2\rangle$, or $|3\rangle$, respectively:

$$\begin{aligned} \rho_W^* \rho_W + \beta_W^* \beta_W + \tau_W^* \tau_W + \alpha_W^* \alpha_W &= 1, \\ \left(\frac{1}{2}\right) \left(\frac{1}{2}\right) + \left(\frac{1}{2}\right) \left(\frac{1}{2}\right) + \left(\frac{1}{2}\right) \left(\frac{1}{2}\right) + \left(\frac{1}{2}\right) \left(\frac{1}{2}\right) &= 1, \end{aligned}$$

$$\begin{aligned} \rho_N^* \rho_N + \beta_N^* \beta_N + \tau_N^* \tau_N + \alpha_N^* \alpha_N &= 1, \\ \left(-\frac{1}{2}i\right) \left(\frac{1}{2}i\right) + \left(-\frac{1}{2}\right) \left(-\frac{1}{2}\right) + \left(\frac{1}{2}i\right) \left(-\frac{1}{2}i\right) + \left(\frac{1}{2}\right) \left(\frac{1}{2}\right) &= 1, \end{aligned}$$

$$\begin{aligned} \rho_E^* \rho_E + \beta_E^* \beta_E + \tau_E^* \tau_E + \alpha_E^* \alpha_E &= 1, \\ \left(\frac{1}{2}\right) \left(\frac{1}{2}\right) + \left(-\frac{1}{2}\right) \left(-\frac{1}{2}\right) + \left(\frac{1}{2}\right) \left(\frac{1}{2}\right) + \left(-\frac{1}{2}\right) \left(-\frac{1}{2}\right) &= 1, \end{aligned}$$

$$\rho_S^* \rho_S + \beta_S^* \beta_S + \tau_S^* \tau_S + \alpha_S^* \alpha_S = 1,$$

$$\left(-\frac{1}{2}i\right) \left(\frac{1}{2}i\right) + \left(\frac{1}{2}\right) \left(\frac{1}{2}\right) + \left(\frac{1}{2}i\right) \left(-\frac{1}{2}i\right) + \left(-\frac{1}{2}\right) \left(-\frac{1}{2}\right) = 1.$$

If two signals are input into the four-port directional coupler Chrestenson gate, the conservation of energy causes the inner product of the two produced vectors of coupling coefficients to be zero:

$$\rho_W^* \tau_E + \beta_W^* \alpha_E + \tau_W^* \rho_E + \alpha_W^* \beta_E = 0,$$

$$\left(\frac{1}{2}\right) \left(\frac{1}{2}\right) + \left(\frac{1}{2}\right) \left(-\frac{1}{2}\right) + \left(\frac{1}{2}\right) \left(\frac{1}{2}\right) + \left(\frac{1}{2}\right) \left(-\frac{1}{2}\right) = 0,$$

$$\alpha_N^* \beta_S + \rho_N^* \tau_S + \beta_N^* \alpha_S + \tau_N^* \rho_S = 0,$$

$$\left(\frac{1}{2}\right) \left(\frac{1}{2}\right) + \left(-\frac{1}{2}i\right) \left(-\frac{1}{2}i\right) + \left(-\frac{1}{2}\right) \left(-\frac{1}{2}\right) + \left(\frac{1}{2}i\right) \left(\frac{1}{2}i\right) = 0,$$

$$\rho_W^* \alpha_N + \beta_W^* \rho_N + \tau_W^* \beta_N + \alpha_W^* \tau_N = 0,$$

$$\left(\frac{1}{2}\right) \left(\frac{1}{2}\right) + \left(\frac{1}{2}\right) \left(\frac{1}{2}i\right) + \left(\frac{1}{2}\right) \left(-\frac{1}{2}\right) + \left(\frac{1}{2}\right) \left(-\frac{1}{2}i\right),$$

$$\alpha_N^* \tau_E + \rho_N^* \alpha_E + \beta_N^* \rho_E + \tau_N^* \beta_E = 0,$$

$$\left(\frac{1}{2}\right) \left(\frac{1}{2}\right) + \left(-\frac{1}{2}i\right) \left(-\frac{1}{2}\right) + \left(-\frac{1}{2}\right) \left(\frac{1}{2}\right) + \left(\frac{1}{2}i\right) \left(-\frac{1}{2}\right) = 0,$$

$$\tau_E^* \beta_S + \alpha_E^* \tau_S + \rho_E^* \alpha_S + \beta_E^* \rho_S = 0,$$

$$\left(\frac{1}{2}\right) \left(\frac{1}{2}\right) + \left(-\frac{1}{2}\right) \left(-\frac{1}{2}i\right) + \left(\frac{1}{2}\right) \left(-\frac{1}{2}\right) + \left(-\frac{1}{2}\right) \left(\frac{1}{2}i\right) = 0,$$

$$\rho_W^* \beta_S + \beta_W^* \tau_S + \tau_W^* \alpha_S + \alpha_W^* \rho_S = 0,$$

$$\left(\frac{1}{2}\right) \left(\frac{1}{2}\right) + \left(\frac{1}{2}\right) \left(-\frac{1}{2}i\right) + \left(\frac{1}{2}\right) \left(-\frac{1}{2}\right) + \left(\frac{1}{2}\right) \left(\frac{1}{2}i\right) = 0.$$

Since these equations are satisfied with the elements of the derived radix-4 Chrestenson transform matrix, the four-port directional coupler proves to act as an effective radix-4 Chrestenson gate.

VI. CONCLUSION

In this paper, an integrated photonic four-port directional coupler that has potential for integration in radix-4 qudit based quantum photonic circuits is discussed. By showing that the radix-4 Chrestenson transfer function satisfies the operational conditions imposed by the conservation of energy for the coupler, we demonstrate the component's ability to act as a radix-4 qudit Chrestenson gate in an optical quantum system. The Chrestenson gate puts a radix- p qudit into a state of equal superposition between all orthogonal basis states, so the discovery of a physical realization of such a gate is significant. Because a linear combination of radix-4 basis states can be achieved in quantum optics whenever the four-port coupler is used, QIP algorithms that utilize qudit superposition can be

realized with this element. The introduction of new quantum applications for the four-port directional coupler as a radix-4 Chrestenson gate will lead to additional gates and methods that make radix-4 optical systems more robust.

REFERENCES

- [1] D. P. DiVincenzo, "The Physical Implementation of Quantum Computation," *Fortschritte der Physik*, vol. 48, no. 9-11, pp. 771-783, 2000.
- [2] M. A. Nielsen and I. L. Chuang, *Quantum Computation and Quantum Information*, Cambridge University Press, 2010.
- [3] D. Deutsch, "Quantum theory, the Church-Turing principle and the universal quantum computer," *Proceedings of the Royal Society of London A: Mathematical, Physical and Engineering Sciences*, vol. 400, no. 1818, pp. 97-117, 1985.
- [4] D. L. MacFarlane, J. Tong, C. Fafadia, V. Govindan, L. R. Hunt, and I. Panahi, "Extended lattice filters enabled by four-directional couplers," *Applied Optics*, vol. 43, no. 33, pp. 6124-6133, 2004.
- [5] K. Fujii, "Quantum optical construction of generalized Pauli and Walsh-Hadamard matrices in three level systems," *arXiv preprint quant-ph/0309132*, 2003.
- [6] N. Y. Vilenkin, "Concerning a class of complete orthogonal systems," *Dokl. Akad. Nauk SSSR, Ser. Math.*, no. 11, 1947.
- [7] H. E. Chrestenson, "A class of generalized Walsh functions," *Pacific Journal of Mathematics*, vol. 5, pp. 17-31, 1955.
- [8] Z. Zilic and K. Radecka, "Scaling and better approximating quantum Fourier transform by higher radices," *IEEE Trans. on Computers*, vol. 56, no. 2, pp. 202-207, 2007.
- [9] P. Kok, W. J. Munro, K. Nemoto, T. C. Ralph, J. P. Dowling, and G. J. Milburn, "Linear optical quantum computing with photonic qubits," *Reviews of Modern Physics*, vol. 79, no. 1, pp. 135-174, 2007.
- [10] E. Knill, R. Laflamme, and G. J. Milburn, "A scheme for efficient quantum computation with linear optics," *Nature*, vol. 409, no. 6816, pp. 46-52, 2001.
- [11] J. Eisert, "Optimizing linear optics quantum gates," *Physical review letters*, vol. 95, no. 4, 2005.
- [12] D. L. MacFarlane, M. P. Christensen, K. Liu, T. P. LaFave Jr., G. A. Evans, N. Sultana, T. W. Kim, J. Kim, J. B. Kirk, N. Huntoon, A. J. Stark, M. Dabkowski, L. R. Hunt, and V. Ramakrishna, "Four-port nanophotonic frustrated total-internal reflection coupler," *IEEE Phot. Tech. Lett.*, vol. 24, no. 1, pp. 58-60, 2012.
- [13] D. L. MacFarlane, M. P. Christensen, A. El Nagdi, G. A. Evans, L. R. Hunt, N. Huntoon, J. Kim, T. W. Kim, J. Kirk, T. P. LaFave Jr., K. Liu, V. Ramakrishna, M. Dabkowski, and N. Sultana, "Experiment and theory of an active optical filter," *IEEE J. Quant. Electron.*, vol. 48, no. 3, pp. 307-317, 2012.
- [14] D. S. Gale, "Frustrated total internal reflection," *Am. J. Phys.*, vol. 40, no. 7, pp. 1038-1039, 1972.
- [15] N. Sultana, W. Zhou, T. LaFave Jr and D. L. MacFarlane "HBr based inductively coupled plasma etching of high aspect ratio nanoscale trenches in InP: Considerations for photonic applications," *J. Vac. Sci. B* vol. 27, no. 6, pp. 2351-2356, 2009.
- [16] J. C. García-Escartín and P. Chamorro-Posada, "Quantum multiplexing with the orbital angular momentum of light," *Physical Review A*, vol. 78, no. 6, 2008.